

Numerical Simulation of Forging Process Using the Hybrid PCM/FEM

YONG-MING GUO

Department of Mechanical Engineering
Graduate School of Science and Engineering, Kagoshima University
1-21-40 Korimoto, Kagoshima City, 890-0065
JAPAN

guoy@mech.kagoshima-u.ac.jp <http://www.mech.kagoshima-u.ac.jp/eng/index.html>

Abstract: - In this paper, for analyses of metal forming problems, a point collocation method (PCM) with a boundary layer of finite element is developed. PCMs have some advantages such as no mesh, no integration. While, the robustness of the PCMs is an issue especially when scattered and random points are used. To improve the robustness, some studies suggest that the positivity conditions can be important when using the PCMs. For boundary points, however, the positivity conditions cannot be satisfied, so that it is possible to get large numerical errors from the boundary points when using the PCMs. Specifically, the errors could arise in point collocation analyses with complicated boundary conditions. In this paper, by introducing a boundary layer of finite element in boundary domain of workpiece, unsatisfactory issue of the positivity conditions of boundary points can be avoided, and the complicated boundary conditions can be easily imposed with the boundary layer of finite element. A forging process is analyzed by using the hybrid PCM/FEM.

Key-Words: - Meshless method, Point collocation method, Positivity conditions, FEM, Hybrid method, Forging

1 Introduction

Meshless methods have found application in many references. The early representatives of meshless methods are the diffuse element method [1], the element free Galerkin method [2], the reproducing kernel particle method [3], the hp-clouds method [4], the partition of unity method [5], the finite point method [6], the local boundary integral equation method [7], the meshless local Petrov-Galerkin (MLPG) approach [8], and the point collocation method (PCM) based on reproducing kernel approximations [9]. Some meshless methods are based on weak form, in which background meshes are inevitable in implementation to obtain the numerical integration. Some meshless methods are truly meshless methods, in which no background meshes are introduced. In most meshless techniques, however, complicated non-polynomial interpolation functions are used which render the integration of the weak form rather difficult. Failure to perform the integration accurately results in loss of accuracy and possibly stability of solution scheme. The integration of complicated non-polynomial interpolation function costs much CPU time, too.

The PCM is a kind of truly meshless method, and has no issues of the integration scheme, the integration accuracy and the integration CPU time. Therefore, the

PCM has some advantages such as no mesh, no integration. Several PCMs based on different types of approximations or interpolations have been presented in the literature. Onate et al. [6] have proposed a finite point method based on weighted least squares interpolations for the analyses of convective transport and fluid flow problems. Onate et al. [10] have also proposed a residual stabilization procedure, adequate for the finite point method, and further extended the finite point method to the solution of the advective-convective transport equations as well as those governing the flow of compressible fluids. Aluru [9] has presented a PCM based on reproducing kernel approximations for numerical solution partial differential equations with appropriate boundary conditions. Jin, Li and Aluru [11] have shown the robustness of collocation meshless methods can be improved by ensuring that the positivity conditions are satisfied when constructing approximation functions and their derivatives. Wang and Takao [12] have proposed an isoparametric finite point method based on the concept of local isoparametric interpolation. Boroomand, Tabatabaei and Onate [13] have presented a stabilized version of the finite point method to eliminate the ill-conditioning effect due to directional arrangement of the points. Patricio and Rosa [14] have given a numerical solution of a singularly perturbed two-point boundary-value problem using collocation.

Atluri, Liu and Han [15] have presented a MLPG mixed collocation method by using the Dirac delta function as the test function in the MLPG method, and shown that the MPLG mixed collocation method is more efficient than the other MLPG implementations, including the MLPG finite volume method. Atluri, Liu and Han [16] have proposed a finite difference method, within the framework of the MLPG approach, for solving solid mechanics problems. Li and Atluri [17] have demonstrated the suitability and versatility of the MLPG mixed collocation method by solving the problem of topology-optimization of elastic structures. Chantasriwan [18] has provided results of using the multiquadric collocation method to solve the lid-driven cavity flow problem. Wen and Hon [19] have performed a geometrically nonlinear analysis of Reissner-Mindlin plate by using a meshless collocation method based on the smooth radial basis functions. Caraus and Mastrorakis [20], [21] have studied the convergence and the stability of collocation methods for approximate solution of singular integro-differential equations. Kosec and Sarler [22] have explored the application of the mesh-free local radial basis function collocation method in solution of coupled heat transfer and fluid flow problems in Darcy porous media. Wu, Chiu and Wang [23] have developed a mesh-free collocation method based on differential reproducing kernel approximations for the three-dimensional analysis of simply-supported, doubly curved functionally graded magneto-electro-elastic shells under the mechanical load, electric displacement and magnetic flux. Yang et al. [24] have introduced a computational procedure based on meshless generalized finite difference method and serial magnetic resonance imaging data to quantify patient-specific carotid atherosclerotic plaque growth functions and simulate plaque progression. Spanulescu and Moldovan [25] have analyzed the collocation method for solving the Hartree-Fock equations of the self-consistent field in large atomic and molecular systems, and have proposed a method for improving its performances by supplementary analytical and numerical quadrature. Khattak, Tirmizi and Islam [26] have presented an algorithm for the numerical solution of the generalized Hirota-Satsuma equations and Jaulent-Miodek equations based on meshless radial basis functions method using collocation points, called Kansa's method. Hon and Yang [27] have applied the Hermite-based meshless collocation method based on radial basis functions to solve a default barrier model, which is a time-dependent boundary value problem with a singularity at the initial condition. Zahab, Divo

and Kassab [28] have reported on the development and validation of a localized collocation meshless method to model laminar incompressible flows.

While, the robustness of the PCM is an issue especially when scattered and random points are used. To improve the robustness of the PCMs, Nayroles, Touzot and Villon [1] suggested that the positivity conditions could be important when using the PCMs. Jin, Li and Aluru [11] have proposed techniques, based on modification of weighting functions, to ensure satisfaction of positivity conditions when using a scattered set of points. For boundary points, however, the positivity conditions cannot be satisfied, obviously, so that it is possible to get large numerical errors from the boundary points when using the PCMs. Specifically, the errors could arise in point collocation analyses with complicated boundary conditions.

Metal forming problems are nonlinear and large deformation problems. They used to be analyzed by the conventional rigid-plastic finite element methods. But the conventional rigid-plastic finite element methods have some shortcomings as follows: 1) Mesh generation is needed, which is costly. 2) Remeshing is needed when deformation is appreciable, while remeshing results in loss of accuracy.

In this paper, the PCM with a boundary layer of finite element is developed. By introducing a boundary layer of finite element in boundary domain of analyzed body, unsatisfactory issue of the positivity conditions of boundary points can be avoided, and the complicated boundary conditions can be easily imposed with the boundary layer of finite element. In addition, a local coordinate system is used, it renders the shape function and its derivatives of collocated points very simple. An axisymmetric forging process is analyzed by using the hybrid method.

2 Formulation

Let us assume a scalar problem governed by a partial differential equation:

$$D(u) = b, \quad \text{in } \Omega \quad (1)$$

with boundary conditions

$$T(u) = t, \quad \text{on } \Gamma_t \quad (2)$$

$$u - u_c = 0, \quad \text{on } \Gamma_u \quad (3)$$

to be satisfied in a domain Ω with boundary $\Gamma = \Gamma_t \cup \Gamma_u$, where D and T are appropriate differential operators, u is the problem unknown function (the velocity is adopted in this paper), b and t are external forces or sources acting over Ω and along Γ_t ,

respectively. u_c is the assigned value of u over Γ_u .

Let us assume Ω is divided into two subdomains, the interior domain Ω_{in} and the boundary domain Ω_{bo} . Surface between Ω_{in} and Ω_{bo} is defined as S .

2.1 The Moving Least-Squares Approximation

Consider a small domain Ω_x , the neighborhood of a point x_1 , which is located in Ω_{in} . Over Ω_x , u can be approximated by the moving least-squares (MLS) approximation [1]. The MLS approximation with quadratic basis is not sensitive to the number of nodes in a sub-domain [6]. Derivatives of interpolations using the MLS approximation show smaller oscillations than those in the partition of unity method [29]. The MLS approximation has better efficiency than the radial basis point interpolation method [30].

Over a number of randomly located nodes $\{x_i\}, i=1, 2, \dots, n$, the MLS approximation u^h of u can be defined by

$$\mathbf{u}^h = \mathbf{p}^T(\mathbf{x})\boldsymbol{\alpha}, \quad \forall \mathbf{x} \in \Omega_x \quad (4)$$

where $\mathbf{p}^T(\mathbf{x}) = [p_1(\mathbf{x}) \ p_2(\mathbf{x}) \ \dots \ p_m(\mathbf{x})]$ is a complete monomial basis of order m which is functions of the space coordinates $\mathbf{x} = [x \ y \ z]^T$. For example, for an axisymmetric problem in which $\mathbf{x} = [R \ Z]^T$,

$$\mathbf{p}^T(\mathbf{x}) = \begin{bmatrix} 1 & R & Z & R^2 & RZ & Z^2 \end{bmatrix} \quad (5)$$

this is a quadratic basis, and $m=6$.

The coefficient vector $\boldsymbol{\alpha}$ is a vector containing coefficients $\alpha_j, j=1, 2, \dots, m$, and $\boldsymbol{\alpha}$ is determined by minimizing a weighted discrete L_2 norm, defined as:

$$J = \sum_{i=1}^n w(\mathbf{x}_i) \left[\mathbf{p}^T(\mathbf{x}_i)\boldsymbol{\alpha} - \hat{u}_i \right]^2 = [\mathbf{H}\boldsymbol{\alpha} - \hat{\mathbf{u}}]^T \mathbf{W} [\mathbf{H}\boldsymbol{\alpha} - \hat{\mathbf{u}}] \quad (6)$$

where $w(\mathbf{x})$ is the weight function, with $w(\mathbf{x}) > 0$ for all nodes in the support of $w(\mathbf{x})$ (the support is considered to be equal to Ω_x in this paper), \mathbf{x}_i denotes the value of \mathbf{x} at node i , n is the number of nodes in Ω_x , and the matrices \mathbf{W} and \mathbf{H} are defined as

$$\mathbf{W} = \begin{bmatrix} w(\mathbf{x}_1) & 0 & \dots & 0 \\ 0 & w(\mathbf{x}_2) & \dots & 0 \\ \dots & \dots & \dots & \dots \\ 0 & 0 & \dots & w(\mathbf{x}_n) \end{bmatrix}_{n \times n} \quad (7)$$

$$\mathbf{H} = \begin{bmatrix} \mathbf{p}^T(\mathbf{x}_1) \\ \mathbf{p}^T(\mathbf{x}_2) \\ \dots \\ \mathbf{p}^T(\mathbf{x}_n) \end{bmatrix}_{n \times m} \quad (8)$$

and

$$\hat{\mathbf{u}} = [\hat{u}_1 \ \hat{u}_2 \ \dots \ \hat{u}_n]^T \quad (9)$$

where $\hat{u}_i, i=1, 2, \dots, n$ are the fictitious nodal values of the function and not the nodal values of the trial function $\mathbf{u}^h(x_i)$ in general:

$$\hat{u}_i \neq u^h(x_i) \quad (10)$$

Minimizing J in equation (6) with respect to $\boldsymbol{\alpha}$ yields

$$\boldsymbol{\alpha} = \mathbf{A}^{-1} \mathbf{B} \hat{\mathbf{u}} \quad (11)$$

where

$$\mathbf{B} = \mathbf{H}^T \mathbf{W} = [w(\mathbf{x}_1)\mathbf{p}(\mathbf{x}_1) \ w(\mathbf{x}_2)\mathbf{p}(\mathbf{x}_2) \ \dots \ w(\mathbf{x}_n)\mathbf{p}(\mathbf{x}_n)] \quad (12)$$

$$\mathbf{A} = \mathbf{B} \mathbf{H} = \sum_{i=1}^n w(\mathbf{x}_i) \mathbf{p}(\mathbf{x}_i) \mathbf{p}^T(\mathbf{x}_i) \quad (13)$$

Substituting equation (11) into equation (4) gives a relation which may be written as the form of an interpolation function, as

$$\mathbf{u}^h = \mathbf{N}^T(\mathbf{x}) \hat{\mathbf{u}} = \sum_{i=1}^n N_i(\mathbf{x}) \hat{u}_i \quad (14)$$

where

$$\mathbf{N}^T(\mathbf{x}) = \mathbf{p}^T(\mathbf{x}) \mathbf{A}^{-1} \mathbf{B} \quad (15)$$

$$N_i(\mathbf{x}) = \sum_{j=1}^m p_j(\mathbf{x}) [\mathbf{A}^{-1} \mathbf{B}]_{ji} \quad (16)$$

$N_i(\mathbf{x})$ is the shape function of the MLS approximation.

The MLS approximation is well defined only when matrix \mathbf{A} in equation (11) is non-singular. It may be seen that this is the case if and only if the rank of the matrix \mathbf{H} equals m . A necessary condition for a well-defined MLS approximation is that at least m weight functions are non-zero (i.e. $n \geq m$) for each node $\mathbf{x} \in \Omega_x$, and that the nodes in Ω_x will not be arranged in a special pattern.

In this paper, the weight functions $w(\mathbf{x})$ may use a Gaussian function, and the Gaussian function corresponding to node i is defined as

$$w(\mathbf{x}) = \frac{\exp(-(d/c)^2) - \exp(-(r/c)^2)}{1 - \exp(-(r/c)^2)}, \quad 0 \leq d \leq r \quad (17a)$$

$$w(\mathbf{x}) = 0, \quad d \geq r \quad (17b)$$

where $d = |\mathbf{x} - \mathbf{x}_1|$ is the distance from node x to point x_1 , and r is the radius of Ω_x , which is taken as a circle

for a 2-D problem and its center is the point x_1 (the center node). c is a constant.

In Ω_x , the unknown function u can be approximated by the MLS approximation as

$$u(\mathbf{x}) \cong u^h(\mathbf{x}) = \mathbf{N}^T(\mathbf{x})\hat{\mathbf{u}} = \sum_{i=1}^n N_i(\mathbf{x})\hat{u}_i \quad (18)$$

2.2 The Local Coordinate System

As anisotropy of the point distribution in Ω_x , matrix \mathbf{A} in equation (13) becomes ill-conditioned and the quality of the approximation deteriorates. In order to prevent such undesirable effect, a local coordinate system ξ, η [13] is chosen with origin at the point x_1 for an axisymmetric problem:

$$\xi = \frac{R - R_1}{\Delta_R} \quad (19a)$$

$$\eta = \frac{Z - Z_1}{\Delta_Z} \quad (19b)$$

where Δ_R and Δ_Z denote maximum distances along R and Z measured from the point x_1 to exterior nodes in Ω_x . In equation (17a), Gaussian function has now the following form in terms of the local coordinates:

$$w(\xi) = \frac{\exp(-(\xi^2 + \eta^2)/c^2) - \exp(-(\rho/c)^2)}{1 - \exp(-(\rho/c)^2)} \quad (20)$$

$c=0.25$, $\rho=2$ are used in this paper and as usual $-1 \leq \xi \leq 1, -1 \leq \eta \leq 1$.

The matrix \mathbf{A} is not longer dependent on the dimensions of Ω_x . The approximate function is also expressed in terms of the local coordinates as

$$u^h(\xi) = \mathbf{N}^T(\xi)\hat{\mathbf{u}} = \sum_{i=1}^n N_i(\xi)\hat{u}_i \quad (21)$$

Over the boundary domain Ω_{bo} of Ω , the FEM with one layer of finite element is used, the finite element approximation u^g of u can be defined by

$$u^g = [\mathbf{N}^e]^T \mathbf{u}^e = \sum_{i=1}^{n_e} N_i^e u_i^e \quad (22)$$

where N_i^e is the shape function of FEM, and u_i^e is the node value of the finite elements,

$$u_i^e = u^g(x_i) \quad (23)$$

n_e is the number of nodes of an element.

2.3 The Weighted Residual Method

On surface S between Ω_{in} and Ω_{bo} , the following compatibility condition of u is imposed:

$$\mathbf{u}^h = \mathbf{u}^g \quad \text{on } S \quad (24)$$

Over Ω_{in} , the following weighted residual method is used:

$$\int_{\Omega_{in}} \hat{w}_i (D(\mathbf{u}^h) - b) d\Omega + \int_S \tilde{w}_i (\mathbf{u}^h - \mathbf{u}^g) dS = 0 \quad (25)$$

where \hat{w}_i and \tilde{w}_i are two weight functions.

Substituting equations on \mathbf{u}^h and \mathbf{u}^g into equation (25), the following equation may be obtained:

$$\int_{\Omega_{in}} \hat{w}_i (D(\hat{\mathbf{u}}) - b) d\Omega + \int_S \tilde{w}_i (\mathbf{N}^T \hat{\mathbf{u}} - [\mathbf{N}^e]^T \mathbf{u}^e) dS = 0 \quad (26)$$

\hat{w}_i and \tilde{w}_i may be defined as follow in this paper, respectively.

$$\hat{w}_i = \delta_i \quad (27)$$

$$\tilde{w}_i = \delta_i \quad (28)$$

where δ_i is Dirac δ function.

Substituting equations (27) and (28) into equation (26), the following equations are obtained:

$$D(\hat{\mathbf{u}}) - b = 0, \quad \text{in } \Omega_{in} \quad (29)$$

$$D(\hat{\mathbf{u}}) - b + [\mathbf{N}^T \hat{\mathbf{u}} - \mathbf{u}^e] = 0 \quad \text{on } S \quad (30)$$

The boundary conditions of equations (2) and (3) are imposed by using FEM.

2.4 The Positivity Conditions

The positivity conditions [11] on the approximation function $N_i(\mathbf{x})$ of equation (16) and its second-order derivatives are stated as

$$N_i(\mathbf{x}_j) \geq 0 \quad (31)$$

$$\nabla^2 N_i(\mathbf{x}_j) \geq 0, \quad j \neq i \quad (32)$$

$$\nabla^2 N_i(\mathbf{x}_i) < 0 \quad (33)$$

where $N_i(\mathbf{x}_j)$ is the approximation function of a point i evaluated at a point j .

It has been shown that the satisfaction of the positivity conditions ensures the convergence of the finite difference method with arbitrary irregular meshes for some class of elliptic problems [31]. It has been shown that the significance of the positivity conditions in meshless collocation approaches, and violation of the positivity conditions can significantly result in a large error in the numerical solution [11].

For a boundary point, a neighborhood centered on the point cannot be defined, so the positivity conditions

on the boundary point cannot be satisfied. But for point x on S , because it is not a boundary point, a small domain Ω_x , the neighborhood of the point x , can be defined. Therefore, the unsatisfactory issue of the positivity conditions of boundary points can be avoided in the hybrid PCM/FEM.

2.5 Formulation for Metal Forming Problems

For an axisymmetric metal forming problem, the partial differential equations of mechanical equilibrium can be expressed as (in this paper, the body forces are omitted for simplicity):

$$\frac{\partial \sigma_R}{\partial R} + \frac{\partial \sigma_{RZ}}{\partial Z} + \frac{\sigma_R - \sigma_\theta}{R} = 0 \quad (34a)$$

$$\frac{\partial \sigma_{RZ}}{\partial R} + \frac{\partial \sigma_Z}{\partial Z} + \frac{\sigma_{RZ}}{R} = 0 \quad (34b)$$

where $\sigma_R, \sigma_Z, \sigma_\theta$ and σ_{RZ} are stress components. By the concept referring originally to a (nonlinear) viscous solid, the relating equation of stress vector σ and strain rate vector $\dot{\epsilon}$ can be written as:

$$\sigma = \mathbf{D} \dot{\epsilon} \quad (35)$$

for the rigid-plastic material

$$\mathbf{D} = \frac{\sigma_e}{\dot{\epsilon}_e} \left[\frac{1}{3} \begin{bmatrix} 2 & 0 & 0 & 0 \\ 0 & 2 & 0 & 0 \\ 0 & 0 & 2 & 0 \\ 0 & 0 & 0 & 1 \end{bmatrix} + \left(\frac{1}{g} - \frac{2}{9} \right) \begin{bmatrix} 1 & 1 & 1 & 0 \\ 1 & 1 & 1 & 0 \\ 1 & 1 & 1 & 0 \\ 0 & 0 & 0 & 0 \end{bmatrix} \right] \quad (36)$$

where σ_e and $\dot{\epsilon}_e$ denote the equivalent stress and the equivalent strain rate, respectively, and g is a material constant and a function of material density for slightly compressible materials.

Substituting the relationship equation of velocity and strain rate into equation (35), and then equations (34a) and (34b), the following non-linear equation of the mechanical equilibrium is derived:

$$\nabla^2 \mathbf{u} + \mathbf{f} = \mathbf{0} \quad (37)$$

in which \mathbf{u} is the velocity vector:

$$\mathbf{u} = [u \quad v]^T \quad (38)$$

$$\mathbf{f} = [f_R \quad f_Z]^T \quad (39)$$

where u and v denote velocity components, and

$$f_R = \left(\frac{3}{g} + \frac{1}{3} \right) \frac{\partial \dot{\epsilon}_v}{\partial R} + \frac{1}{R} (\dot{\epsilon}_R - \dot{\epsilon}_\theta) + \left(\frac{1}{\sigma_e} \frac{\partial \sigma_e}{\partial R} - \frac{1}{\dot{\epsilon}_e} \frac{\partial \dot{\epsilon}_e}{\partial R} \right) \left[2\dot{\epsilon}_R + \left(\frac{3}{g} - \frac{2}{3} \right) \dot{\epsilon}_v \right] + \left(\frac{1}{\sigma_e} \frac{\partial \sigma_e}{\partial Z} - \frac{1}{\dot{\epsilon}_e} \frac{\partial \dot{\epsilon}_e}{\partial Z} \right) \dot{\gamma}_{RZ} \quad (40a)$$

$$f_Z = \left(\frac{3}{g} + \frac{1}{3} \right) \frac{\partial \dot{\epsilon}_v}{\partial Z} + \frac{1}{R} \frac{\partial v}{\partial R} + \left(\frac{1}{\sigma_e} \frac{\partial \sigma_e}{\partial Z} - \frac{1}{\dot{\epsilon}_e} \frac{\partial \dot{\epsilon}_e}{\partial Z} \right) \left[2\dot{\epsilon}_Z + \left(\frac{3}{g} - \frac{2}{3} \right) \dot{\epsilon}_v \right] + \left(\frac{1}{\sigma_e} \frac{\partial \sigma_e}{\partial R} - \frac{1}{\dot{\epsilon}_e} \frac{\partial \dot{\epsilon}_e}{\partial R} \right) \dot{\gamma}_{RZ} \quad (40b)$$

where $\dot{\epsilon}_v$ is the volumetric strain rate:

$$\dot{\epsilon}_v = \dot{\epsilon}_R + \dot{\epsilon}_Z + \dot{\epsilon}_\theta \quad (41)$$

Over Ω_{in} , by the MLS approximation, \mathbf{u} in equation (37) can be written as:

$$u = \mathbf{N}^T \hat{\mathbf{u}} \quad (42a)$$

$$v = \mathbf{N}^T \hat{\mathbf{v}} \quad (42b)$$

Substituting equation (37) into equations (29) and (30), the partial differential equations on the nodal velocity components may be obtained:

$$\nabla^2 \mathbf{N}^T \hat{\mathbf{u}} + \mathbf{f}(\hat{\mathbf{u}}, \hat{\mathbf{v}}) = 0 \quad \text{in } \Omega_{in} \quad (43a)$$

$$\nabla^2 \mathbf{N}^T \hat{\mathbf{v}} + \mathbf{f}(\hat{\mathbf{u}}, \hat{\mathbf{v}}) = 0 \quad \text{in } \Omega_{in} \quad (43b)$$

$$\nabla^2 \mathbf{N}^T \hat{\mathbf{u}} + \mathbf{f}(\hat{\mathbf{u}}, \hat{\mathbf{v}}) + [\mathbf{N}^T \hat{\mathbf{u}} - \mathbf{u}^e] = 0 \quad \text{on } S \quad (44a)$$

$$\nabla^2 \mathbf{N}^T \hat{\mathbf{v}} + \mathbf{f}(\hat{\mathbf{u}}, \hat{\mathbf{v}}) + [\mathbf{N}^T \hat{\mathbf{v}} - \mathbf{v}^e] = 0 \quad \text{on } S \quad (44b)$$

In Ω_{bo} , the rigid-plastic FEM with one layer of finite element is used, and the boundary conditions of forming problems are imposed on Γ by using the rigid-plastic FEM, too.

3 Analyzed Results of the Forging Process

In this section, an axisymmetric forging problem (see Fig.1) is analyzed. Material constant g is taken as 0.007. Coulomb friction is used, and the friction factor is taken

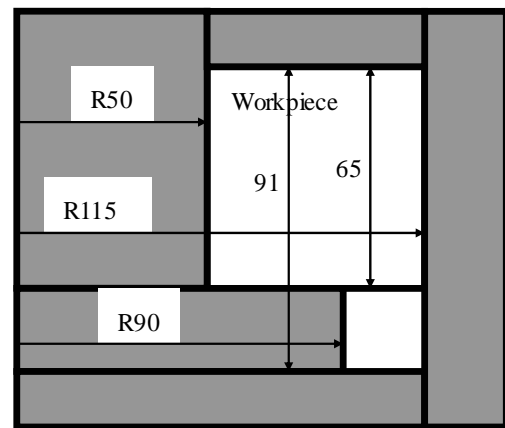


Fig. 1. Initial shape and dimensions of the workpiece and dies.

as 0.1. Forging velocity of the upper die is 0.0065m/s , and increment of time is taken as 0.1 s . The MLS approximation with the quadratic basis ($m=6$) is used. The nodal numbers n and n_e are taken as 9 and 4, respectively.

Figs. 2, 3 and 4 show fields of the nodal velocity in the 10th, 16th and 20th computing step, respectively. As seen in these figures, the field of nodal velocity in the 20th computing step is similar to that in the 10th and 16th computing step. The nodal velocities of lower corner of the inner radius zone are small, and this corner is a dead metal zone.

Figs. 5, 6 and 7 show contours of equivalent strain in the 10th, 15th and the 22nd computing step, respectively. As seen in these figures, the equivalent strains in the 22nd computing step are much larger than those in the 10th and 15th computing step.

Figs. 8, 9 and 10 show contours of equivalent stress in the 10th, 16th and the 20th computing step, respectively. As seen in these figures and Figs. 5, 6 and 7, the distribution of equivalent stress is similar to that of equivalent strain, and the equivalent stresses in the 20th computing step are larger than those in the 10th and 16th computing step.

Figs. 11, 12 and 13 show contours of shear stress in the 8th, 12th and the 15th computing step, respectively.

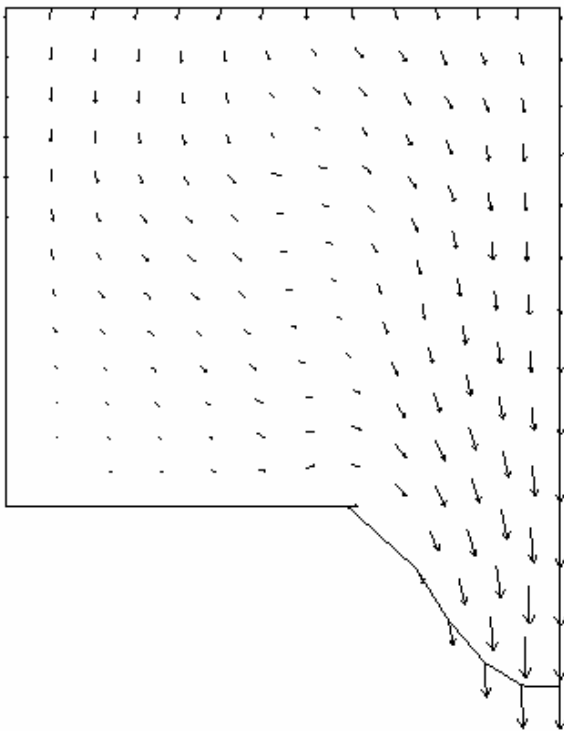


Fig. 2. Nodal velocity field in the 10th computing step.

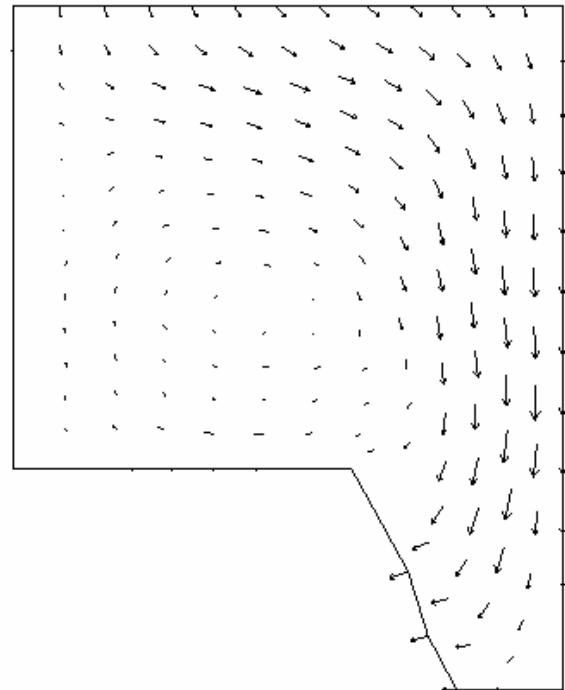


Fig. 3. Nodal velocity field in the 16th computing step.

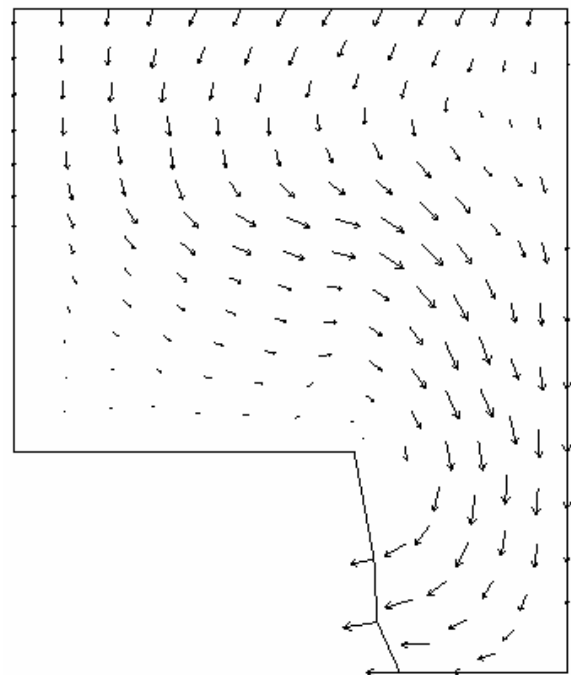


Fig. 4. Nodal velocity field in the 20th computing step.

As seen in these figures, the distribution of shear stress in the 15th computing step is similar to that in

the 8th and 12th computing step.

4 Conclusion

In some point collocation methods, the positivity conditions of boundary points cannot be satisfied, so that it is possible to get large numerical errors from the boundary points. Specifically, the errors could arise in meshless analyses of metal forming problems which have complicated boundary conditions. By introducing a boundary layer of finite element in boundary domain of analyzed body, unsatisfactory issue of the positivity conditions of boundary points in the point collocation methods can be avoided, and the complicated boundary conditions can be easily imposed with the boundary layer of finite element. By making such an improvement, the hybrid PCM/FEM can be used for analyzing problems of metal forming effectively. In this paper, an axisymmetric forging process has been analyzed by using the point collocation method with a boundary layer of finite element, the nodal velocity field, the contours of equivalent strain and shear stress have been obtained successfully.

References:

[1] B. Nayroles, G. Touzot and P. Villon, Generalizing

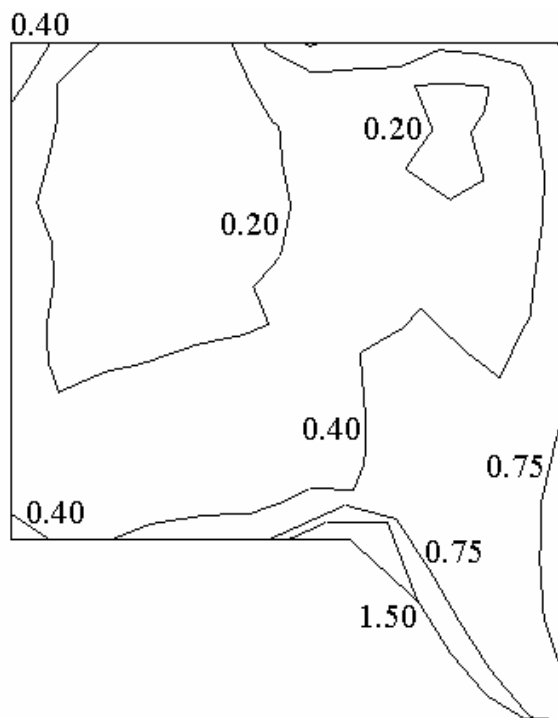


Fig. 5. Contours of equivalent strain in the 10th computing step.

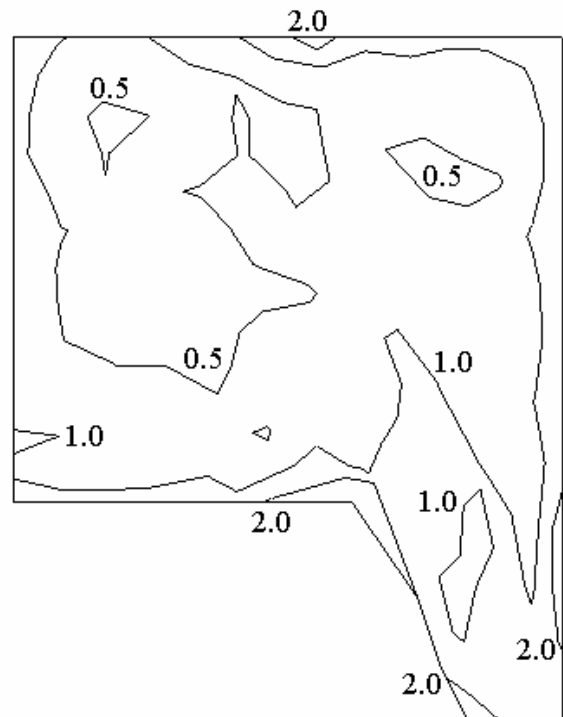


Fig. 6. Contours of equivalent strain in the 15th computing step.

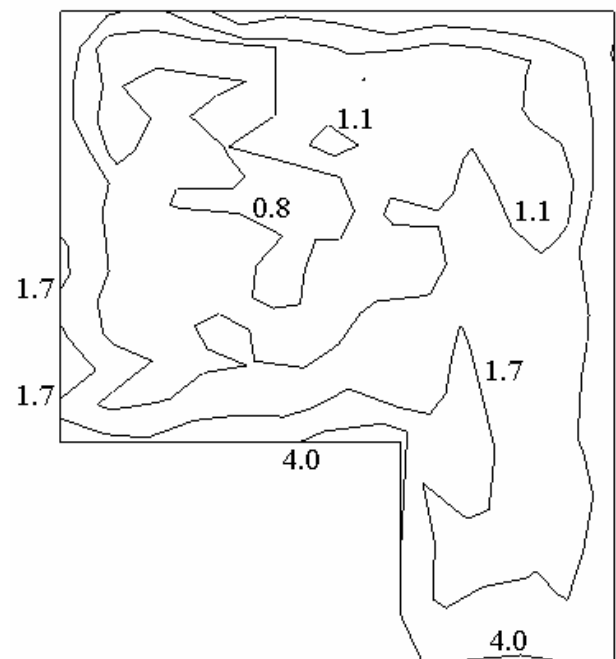


Fig. 7. Contours of equivalent strain in the 22nd computing step.

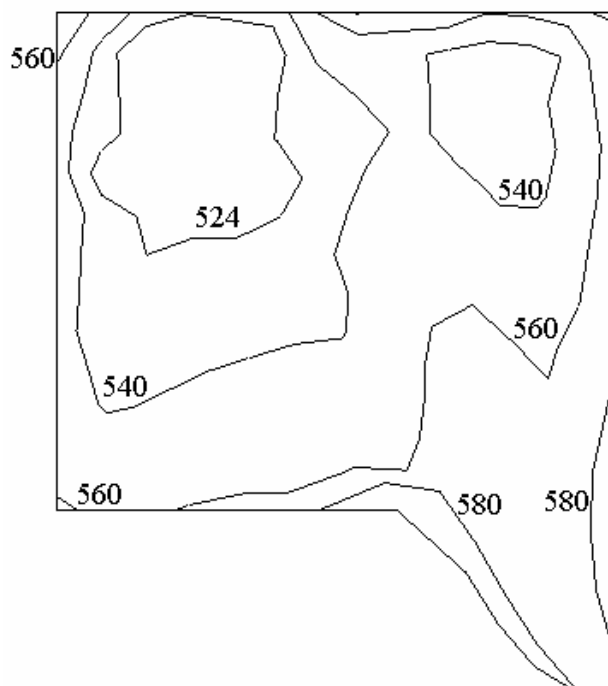


Fig. 8. Contours of equivalent stress (MPa) in the 10th computing step.

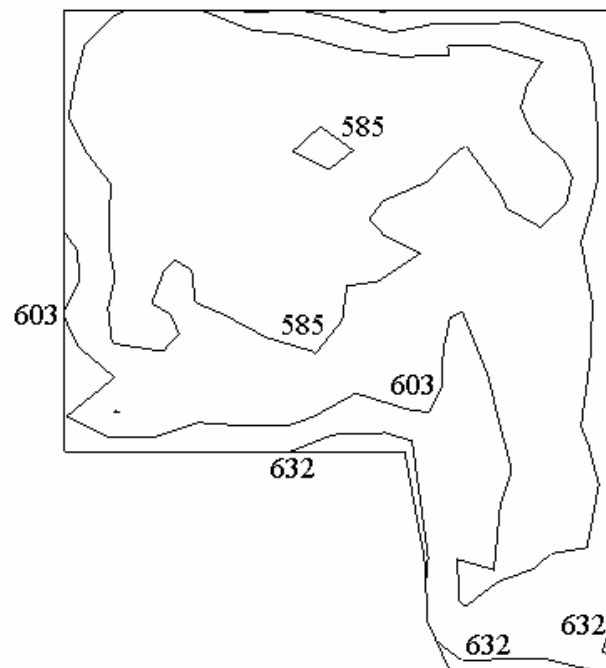


Fig. 10. Contours of equivalent stress (MPa) in the 20th computing step.

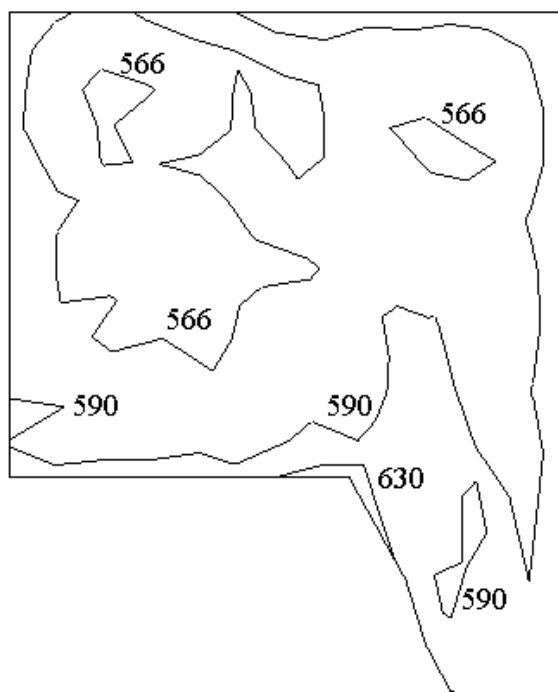


Fig. 9. Contours of equivalent stress (MPa) in the 16th computing step.

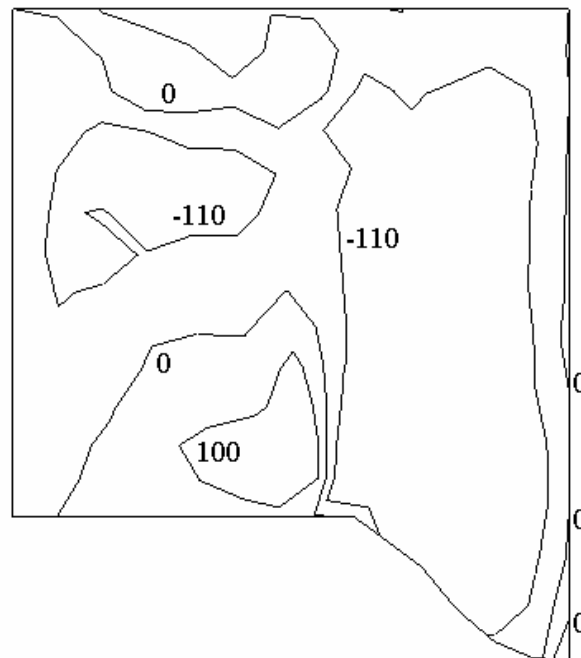


Fig. 11. Contours of shear stress (MPa) in the 8th computing step.

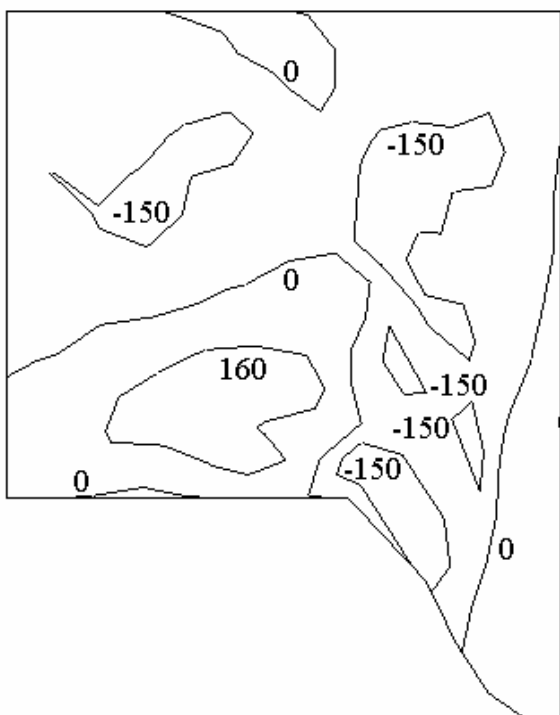


Fig. 12. Contours of shear stress (MPa) in the 12th computing step.

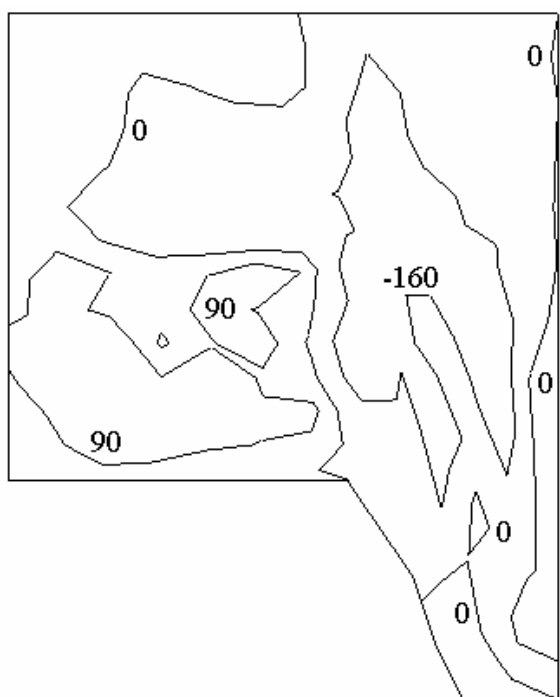


Fig. 13. Contours of shear stress (MPa) in the 15th computing step.

the FEM: diffuse approximation and diffuse elements, *Computational Mechanics*, Vol.10, 1992, pp.307-318.

- [2] T. Belytschko, Y. Y. Lu and L. Gu, Element free Galerkin methods, *Int. J. Numer. Methods Engrg.*, Vol.37, 1994, pp.229-256.
- [3] W. K. Liu, S. Jun, S. Li, J. Adee and T. Belytschko, Reproducing kernel particle methods for structural dynamics, *Int. J. Numer. Methods Engrg.*, Vol.38, 1995, pp.1655-1679.
- [4] C. A. Duarte and J. T. Oden, An h-p adaptive method using clouds, *Comput. Methods Appl. Mech. Engrg.*, Vol.139, 1996, pp.237-262.
- [5] J. M. Melenk and I. Babuska, The partition of unity finite element method: basic theory and applications, *Comput. Methods Appl. Mech. Engrg.*, Vol.139, 1996, pp.289-314.
- [6] E. Onate, S. Idelsohn, O.C. Zienkiewicz and R.L. Taylor, A finite point method in computational mechanics, *Int. J. Numer. Methods Engrg.*, Vol.39, 1996, pp.3839-3866.
- [7] T. Zhu, J. Zhang and S. N. Atluri, A local boundary integral equation (LBIE) method in computational mechanics and a meshless discretization approach, *Computational Mechanics*, Vol.21, 1998, pp.223-235.
- [8] S. N. Atluri and T. Zhu, A new meshless local Petrov-Galerkin (MLPG) approach in computational mechanics, *Computational Mechanics*, Vol.22, 1998, pp.117-127.
- [9] N. R. Aluru, A point collocation method based on reproducing kernel approximations, *Int. J. Numer. Methods Engrg.*, Vol.47, 2000, pp.1083-1121.
- [10] E. Onate, S. Idelsohn, O. C. Zienkiewicz, R. L. Taylor and C. Sacco, A stabilized finite point method for analysis of fluid mechanics problems, *Comput. Methods Appl. Mech. Engrg.*, Vol.139, 1996, pp.315-346.
- [11] X. Jin, G. Li and N.R. Aluru, Positivity conditions in meshless collocation methods, *Comput. Methods Appl. Mech. Engrg.*, Vol.193, 2004, pp.1171-1202.
- [12] W. X. Wang and Y. Takao, Isoparametric finite point method in computational mechanics, *Computational Mechanics*, Vol.33, 2004, pp.481-490.
- [13] B. Boroomand, A.A. Tabatabaci and E. Onate, Simple modifications for stabilization of the finite point method, *Int. J. Numer. Methods Engrg.*, Vol.63, 2005, pp.351-379.
- [14] M. F. Patricio and P. M. Rosa, Numerical solution of a singularly perturbed two-point

- boundary-value problem using collocation, *Proc. 8th WSEAS Int. Conf. Applied Mathematics*, 2005, pp.25-30.
- [15] S. N. Atluri, H. T. Liu and Z. D. Han, Meshless local Petrov-Galerkin (MPLG) mixed collocation method for elasticity problems, *Computer Modeling Engrg. Sciences*, Vol.14, 2006, pp.141-152.
- [16] S. N. Atluri, H. T. Liu and Z. D. Han, Meshless local Petrov-Galerkin (MPLG) mixed finite difference method for solid mechanics, *Computer Modeling Engrg. Sciences*, Vol.15, 2006, pp.1-16.
- [17] S. Li and S. N. Atluri, Topology-optimization of structures based on the MPLG mixed collocation method, *Computer Modeling Engrg. Sciences*, Vol.26, 2008, pp.61-74.
- [18] S. Chantasiriwan, Performance of multiquadric collocation method in solving lid-driven cavity flow problem with low Reynolds number, *Computer Modeling Engrg. Sciences*, Vol.15, 2006, pp.137-146.
- [19] P. H. Wen and Y. C. Hon, Geometrically nonlinear analysis of Reissner-Mindlin Plate by meshless computation, *Computer Modeling Engrg. Sciences*, Vol.21, 2007, pp.177-191.
- [20] I. Caraus and N. E. Mastorakis, Convergence of the collocation methods for singular integro-differential equations in Lebesgue spaces, *WSEAS Trans. Mathematics*, Vol.6, 2007, pp.859-864.
- [21] I. Caraus and N. E. Mastorakis, The stability of the collocation methods for approximate solution of singular integro-differential equations, *WSEAS Trans. Mathematics*, Vol.7, 2008, pp.121-129.
- [22] G. Kosec and B. Sarler, Local RBF collocation method for Darcy flow, *Computer Modeling Engrg. Sciences*, Vol.25, 2008, pp.197-207.
- [23] C.-P. Wu, K.-H. Chiu and Y.-M. Wang, A mesh-free DRK-based collocation method for the coupled analysis of functionally graded magneto-electro-elastic shells and plates, *Computer Modeling Engrg. Sciences*, Vol.35, 2008, pp.181-214.
- [24] C. Yang, D. Tang, C. Yuan, W. Kerwin, F. Liu, G. Canton, T. S. Hatsukami and S. N. Atluri, Meshless generalized finite difference method and human carotid atherosclerotic plaque progression simulation using multi-year MRI patient-tracking data, *Computer Modeling Engrg. Sciences*, Vol.28, 2008, pp.95-107.
- [25] S. Spanulescu and M. Moldovan, Effects of a supplementary quadrature in the collocation method for solving the Hartree Fock equations in Ab-initio calculations, *WSEAS Trans. Mathematics*, Vol.8, 2009, pp.11-20.
- [26] A. J. Khattak, S. I. A. Tirmizi and S.-ul-Islam, Application of meshfree collocation method to a class of nonlinear partial differential equations, *Engrg. Analysis Boundary Elements*, Vol.33, 2009, pp.661-667.
- [27] Y. C. Hon and Z.-H. Yang, Meshless collocation method by Delta-shaped basis functions for default barrier model, *Engrg. Analysis Boundary Elements*, Vol.33, 2009, pp.951-958.
- [28] Z. El Zahab, E. Divo and A. J. Kassab, A localized collocation meshless method (LCMM) for incompressible flows CFD modeling with applications to transient hemodynamics, *Engrg. Analysis Boundary Elements*, Vol.33, 2009, pp.1045-1061.
- [29] S. N. Atluri, H.G. Kim and J.Y. Cho, A critical assessment of the truly meshless local Petrov-Galerkin (MLPG), and local boundary integral equation (LBIE) methods, *Computational Mechanics*, Vol.24, 1999, pp.348-372.
- [30] G.R. Liu and Y.T. Gu, A meshfree method: meshfree weak-strong (MWS) form method, for 2-D solids, *Computational Mechanics*, Vol.33, 2003, pp.2-14.
- [31] L. Demkowicz, A. Karafilic and T. Liszka, On some convergence results for FDM with irregular mesh, *Comput. Methods Appl. Mech. Engrg.*, Vol.42, 1984, pp.343-355.